Synthesis of highly active H_2O_2-sensitized sulfated titania nanoparticles with a response to visible light

Jian Zou [a,b,*], Jiacheng Gao [a], Yong Wang [a]

[a] College of Materials Science and Engineering, Chongqing University, Chongqing 400044, PR China
[b] School of Chemistry and Chemical Engineering, Southwest University, Chongqing 400715, PR China

ABSTRACT

In this paper, we reported the synthesis of sulfated TiO_2 sensitized with hydrogen peroxide. These prepared TiO_2 showed high photocatalytic activity under the visible light ($\lambda > 420$ nm). X-ray diffraction (XRD), transmission electron micrograph (TEM), UV–vis diffuse reflectance spectroscopy, Fourier transform infrared spectroscopy (FT-IR), BET N_2 adsorption and X-ray photoelectron spectroscopy (XPS) were employed to characterize the properties of the synthesized TiO_2. The results indicated that anatase TiO_2 with strong surface acidity was obtained. The photocatalytic activity of sulfated TiO_2 was compared with that of the commercially available Degussa P25 titanium dioxide by degrading methyl orange (MO) aqueous solutions. The degradation of MO on sulfated TiO_2 under optimal calcining conditions was significantly faster than that on the P25. The active sulfates anchoring on the surface of TiO_2, Ti ions in a tetrahedral coordination and the strong vis absorption may mainly contribute to the high photocatalytic activity of sulfated TiO_2 sensitized with hydrogen peroxide under the visible light.

© 2008 Elsevier B.V. All rights reserved.

1. Introduction

Nanosize TiO_2 particles are used widely as one of the photocatalysts due to their chemical stability, non-toxicity and high activity, but its high activity can be acquired only under ultraviolet light with a wavelength of 400 nm or less at room temperature due to its broad band gap. Since ultraviolet (UV) light is only 3–5% part of the solar spectrum, the photocatalytic activity of TiO_2 cannot be sufficiently activated under solar light irradiation, which limits its application. Therefore, extension of the photoactive wavelength region of TiO_2 into the visible region is desirable for popularizing more TiO_2 photocatalysts, especially under solar light for industrial areas or poor interior lighting illumination in living spaces. For this purpose, pure TiO_2 has been modified by various ways such as impurity doping [1,2], inorganic compound [3] and dye sensitization [4] to obtain visible light reactivity.

The complexes formed on the surfaces of titania particles can be used as another approach to the extension of the photoactive absorption region of TiO_2 photocatalysts into the visible region. Kim et al. [5] recently reported 4-chlorophenol and phenolic compounds in aqueous suspension of pure titania could be degraded under visible illumination. However, the photocatalytic degradation reaction could occur only in the presence of electron acceptors. Hydrogen peroxide was used widely as an electron acceptor in photocatalytic degradation reaction [6,7]. Meanwhile, it is well known that a yellow color appears when the TiO_2 samples are treated with peroxide hydrogen. Although neither hydrogen peroxide nor titania alone can absorb visible light, in the presence of H_2O_2, the –OOH groups of H_2O_2 replace –OH groups on the surface of titania forming yellow surface complexes [8,9], which shift light absorption region to visible light region and color TiO_2 [10]. The coloration of TiO_2 particles by hydrogen peroxide is thought to be related to their photocatalytic activity under visible light. Li et al. [9] have reported that small organic compounds such as salicylic acid were degraded in the presence of P25 TiO_2 and H_2O_2 under visible light, because of the generation of OH radicals from the decomposition of H_2O_2 under visible light irradiation. Ohno et al. [10] also reported rutile showed high vis photocatalytic activity for the photocatalyzed epoxidation of olefin in the presence of H_2O_2, which was consistent with the observations made by others [11]. Besides, hydrogen peroxide can promote formation of active oxygen species [12,13], which are generally contributed to photocatalytic reactions [14].

Recently, many researchers reported that sulfation of TiO_2 could enhance efficiently its photocatalytic activity due to the increase in the fraction of anatase, the surface area, and especially the surface acidity for sulfated TiO_2 [15–18]. In general, the sulfated TiO_2 is obtained by calcining TiO_2 soaked in H_2SO_4. The high calcination temperature is required for high photocatalytic activity for sulfated TiO_2 catalysts [18], due to formation of the strong surface acidity. The strong acid sites on sulfated TiO_2 increase the adsorption

* Corresponding author at: College of Materials Science and Engineering, Chongqing University, Sha Zheng Street, 174, Sha Ping Ba, Chongqing 400044, PR China. Tel.: +86 23 68252361.
E-mail address: ezouj@swu.edu.cn (J. Zou).

strengths and coverages of different organics, which will result in the improved photocatalytic activity [17]. Fu et al. [19] reported the photocatalytic activity of sulfated TiO_2 for the photodegradation of $CHBr_3$, C_6H_6 and C_2H_4 in air was six times higher than that of TiO_2.

Hence, it can be reasonably assumed that the high-vis-active photocatalysts may be obtained by sensitizing sulfated nanosize titania with hydrogen peroxide. To the best of our knowledge, there have been no reports about sulfated TiO_2 sensitized with H_2O_2 as visible-light-active photocatalysts so far. In this work, we reported a simple and efficient method to synthesize sulfated TiO_2 sensitized with H_2O_2. The prepared TiO_2 has high vis photocatalytic activity due to large amount of acidic sites, Ti ions in tetrahedral coordination and strong vis absorption.

2. Experimental

2.1. Preparation of nanosize titania particles

Titanium tetrachloride (Sinopharm Chemical Reagent Co. Ltd., China) was used without any further purification. The titania powders were synthesized by refluxing the $TiCl_4$ aqueous solution containing sulfuric acid. 15 mL titanium tetrachloride was added dropwise into mixture of water and ice, containing 4 mL 98% sulfuric acid under vigorous stirring to make resulting solution 0.5 M in $TiCl_4$. The mixture was kept stirring and boiling to reflux for 4 h and aged for 12 h. Subsequently, the resulting precipitates were separated from the solution by using filtration and repeatedly washed with deionized water to remove the residual chloride ions and its pH value was about 6. Finally, the products were dried at 80 °C for 4 h. The powders were then calcined under various temperatures and durations ranging from 1 to 2 h. All these samples were named sulfated TiO_2 and denoted as TiO_2–T–t, where T refers to calcination temperature and t refers to calcination time. For comparison, commercial Degussa P25 powders were dispersed into deionized water containing the same concentration of sulfuric acid to form the suspension 0.5 M in TiO_2 and boiling to reflux for 1 h and aged for 12 h. The treated P25 suspension was filtrated and dried, and then heat-treated in air at 400 °C for 1 h, and the samples were denoted as P25-S.

The sensitizing TiO_2 was acquired as follows: 1 g TiO_2 powders were dipped and sonicated in 10 mL 30% H_2O_2 for 10 min. The resulting suspension was filtrated and dried at 50 °C temperature for 6 h.

2.2. Characterization

The phase constitutions of the products were characterized through X-ray diffraction method using Cu Kα radiation (λ = 0.15418 nm) in a XD-3 diffractometer (Beijing Pgeneral). Transmission electron microscopy (TEM, Hitachi H7500) was performed at an accelerating voltage of 80 kV for electrons. The BET surface areas of samples were determined by N_2 adsorption–desorption method at 77 K using the 3H-2000I system (Beijing HuiHaiHong Nano-ST). For the adsorption of pyridine, the samples were first dried at 50 °C in vacuum for 2 h and then saturated with pyridine vapor at room temperature for 10 min. Subsequently, the samples were dried at 50 °C in vacuum for 5 h, and the powders with absorption of pyridine were achieved. Fourier transform infrared (FT-IR, Bruker TENSOR 27 FT-IR) spectra of TiO_2 powders were obtained using a spectrometer. The UV–vis spectra were recorded on a spectrophotometer with an integrating sphere (Shmadzu UV-2550); $BaSO_4$ was used as a reference sample. XPS spectrometer (VG Scientific ESCALAB 250) equipped with two ultra-high vacuum (UHV) chambers measurements were performed and all binding energies were referenced to the C_{1s} peak at 284.6 eV of the surface adventitious carbon.

2.3. Measurement of photocatalytic activity and adsorption of methyl orange

The photocatalytic activities of the samples were measured by the degradation of methyl orange (MO, 20 mg L^{-1}) in an aqueous solution. An amount of 0.2 g of sulfated TiO_2 photocatalyst was sonicated with 2 mL 30% hydrogen peroxide for 10 min and suspended in a 200 mL aqueous solution of MO. A 450 W high pressure mercury lamp (Shanghai YaMin) with a filter was used as a visible-light source (λ > 420 nm). Before the photocatalytic experiment, the suspension was stirred in the dark for 30 min and its concentration was original concentration (C_O) of MO. After a given irradiation time, the samples of 5 mL volume were withdrawn, and the catalysts were separated from the suspensions by centrifuging at 5000 r min^{-1}. The concentration (C) of the MO solution was monitored by measuring the maximum absorbance of MO using the UV–vis spectrum.

The reduction in MO concentration due to adsorption was measured by carrying out similar experiment in dark for 30 min. After centrifuging, the pH value of resulted 200 mL MO solution were adjusted to 6–7 by 1 M NaOH. The maximum absorbance of all MO solutions is 464 nm. This concentration was denoted as C_i. The concentration of 20 mg L^{-1} MO was denoted as C_{MO}. The adsorption rate of MO was calculated by the formula $((C_{MO} - C_i)/C_{MO}) \times 100\%$.

3. Results and discussion

3.1. Crystalline structure and morphology

Fig. 1 shows the X-ray powder diffraction (XRD) patterns of the used samples calcined at different conditions. From the XRD patterns, all diffraction peaks can be assigned to the anatase phase without any indication of other crystalline by-products such as rutile or brookite, indicating the formation of pure anatase TiO_2 nanocrystals. The major diffraction peaks of all samples are identical and appear at 2θ values of 25.3°, assigned to the (1 0 1) diffraction planes of anatase TiO_2. In addition, from the diffraction results, it is notable that even titania particles uncalcined (0 °C) are crystalline to some extent. Zhang et al. [20] also reported TiO_2 powder in anatase phase was fabricated without calcination by controlling the hydrolysis of $TiCl_4$ aqueous solution. Meanwhile, the major peak becomes sharper and more intensive as the calcination temperature and time increase, indicating better crystallization.
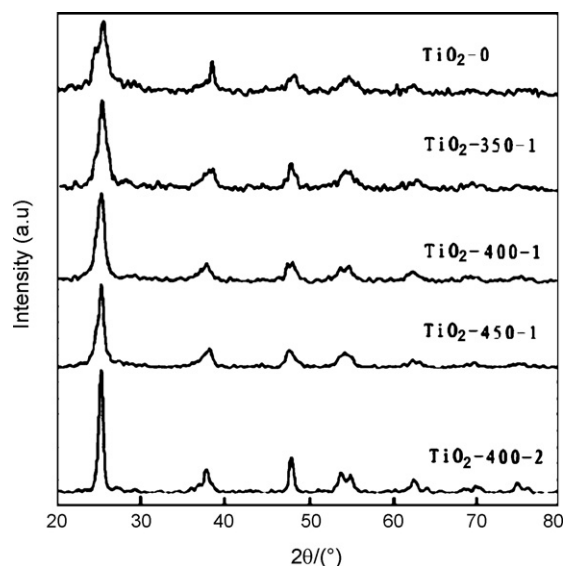

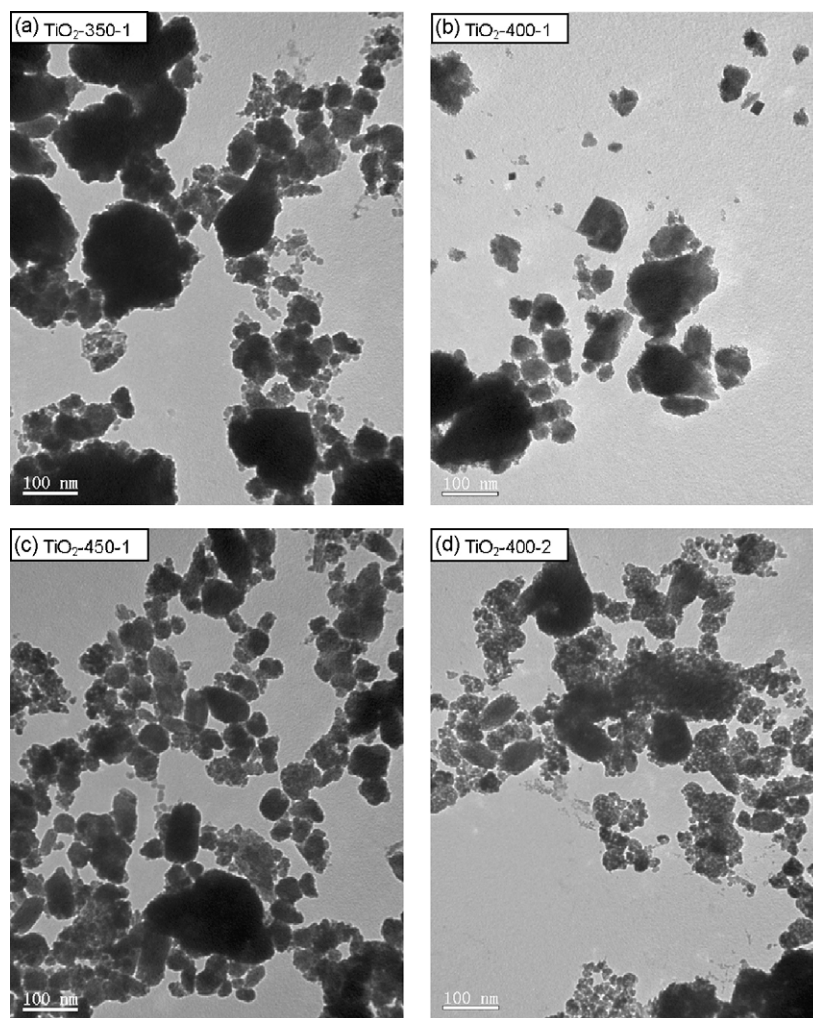**Fig. 1.** XRD spectra of sulfated TiO_2 calcined at different conditions.

Fig. 2. TEM images of sulfated TiO_2 calcined at different conditions.

The average crystallite size has been determined using Scherrer equation, considering the full-width at half-maximum (FWHM) of the maximum intensity diffraction plane (1 0 1), for all the synthesized samples. The calculated crystallite size is found to vary in the range of 6–13 nm in average from 0 to 450 °C. It is clear that the crystallites sizes increase with the increase of the calcination temperature.

The TEM micrographs of sulfated TiO_2 particles are presented in Fig. 2. The crystallites have diameters in the range of 8–13 nm and are aggregated in the size range of 50–300 nm, as shown in Fig. 2. This agglomeration was probably caused by vigorous stirring during hydrolysis of $TiCl_4$ aqueous solution [21]. Calcination makes the aggregates collapse into smaller ones. It is notable that the agglomerations of sample calcined at 350 °C (Fig. 2a) are bigger than those calcined at other temperatures. In addition, some microspores around 3 nm (Fig. 2d) are observed in the agglomerations.

3.2. UV–vis spectra and BET surface areas

The UV–vis spectra of the samples treated and untreated with H_2O_2 are showed in Fig. 3. A new absorption band is observed in the visible range of 400–550 nm in addition to the fundamental absorption edge of TiO_2 (Fig. 3a), located in the UV region (about 400 nm). The calcination temperature is found to have some effects on the vis absorption intensity. The vis absorption decreases with increasing of calcination temperature. Fig. 3a shows that a noticeable decreas-

ing in vis absorption intensity happens to the sample calcined at 400 °C for 2 h, which demonstrates that the influence of calcination time is much greater than that of calcination temperature. The color of sulfated TiO_2 powders changes from white to yellow after they are sensitized with hydrogen peroxide, which is also observed from the P25 powders (Fig. 3b). The vis absorption of the sulfated TiO_2 is more intensive than that of P25, even though the absorption of P25 is shifted to red and increased to some extent after being treated with sulfuric acid and peroxide hydrogen. Therefore, the color of the P25 powders treated with H_2O_2 show pale yellow.

Generally, the color of a solid is determined by the position of its absorption edge. A shift of this absorption edge toward a longer wavelength can result in absorption in the visible part of the spectrum. Fig. 3 shows that neither sulfated TiO_2 nor Degussa P25 can absorb in the visible region, and hydrogen peroxide cannot either. Therefore, many researchers [8–11] attributed the new absorption band to the formation of complexes between surface titanium(IV) and hydrogen peroxide. However, it is noticeable that the vis absorption of sulfated TiO_2 is much stronger than P25. Some researchers think surface area [8,10] and crystal structure [8] influence the absorption, and larger surface area can absorb better. Commonly, surface area decreases with the increase of calcination temperature and time. However, the surface areas of sulfated TiO_2 were observed to increase with the increase of calcination temperature and time (Table 1). As shown from the TEM results (Fig. 2), sulfated TiO_2 powders are presented as some aggregated forms, but agglomeration would break into fragments or form some
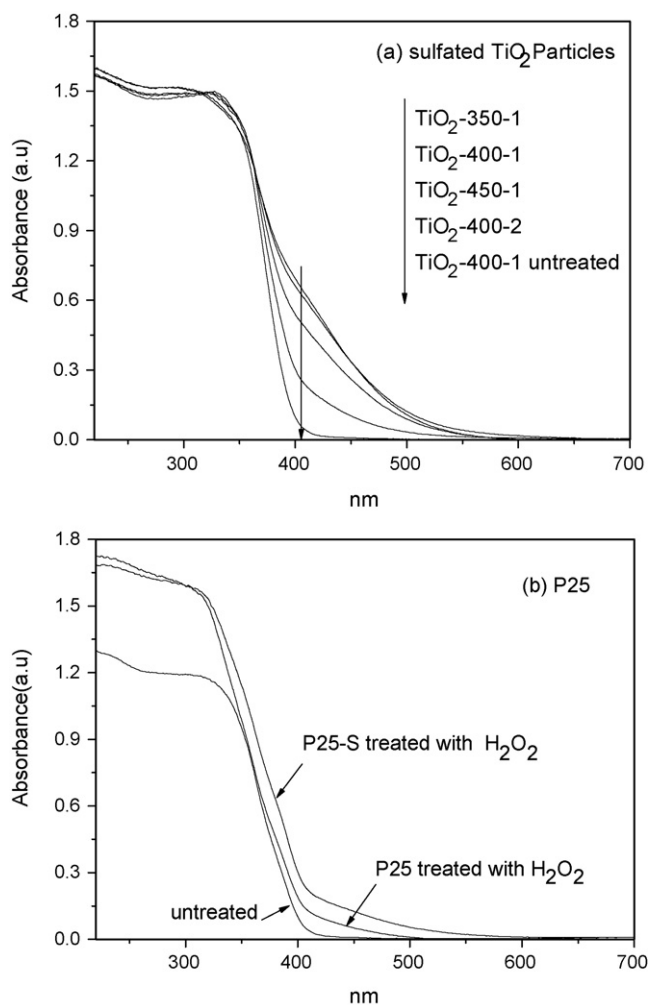
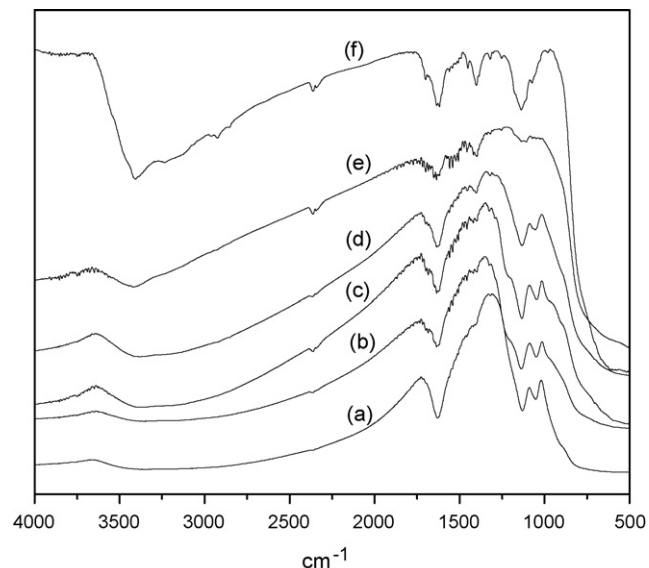Fig. 3. Diffusion reflection absorption of TiO_2 treated with H_2O_2.

Fig. 4. IR spectra of P25 and sulfated TiO_2 particles untreated and treated with H_2O_2: (a) TiO_2–350–1; (b) TiO_2–400–1; (c) TiO_2–400–1 treated with H_2O_2; (d) TiO_2–450–1; (e) P25; (f) TiO_2–400–2.

when sulfated TiO_2 is calcined at below 400 °C. Sulfate species on the surface of sulfated TiO_2 will decompose quickly above 400 °C, so their absorptions decrease with the increase in calcination temperature and duration even though their surface areas become larger. This is consistent with the results shown in Fig. 3a. In fact, it is also supported by the absorption of P25-S powders as shown in Fig. 3b and Table 1 (its absorption is red shifted and becomes stronger, even its surface area is less).

3.3. Composition and chemical structure

Fig. 4 shows IR spectra of P25 and sulfated TiO_2 powders calcined at different conditions. All the samples exhibit the strong absorptions at ~3400 and ~1630 cm^{-1}, which correspond to the surface adsorbed water and the hydroxyl groups [16,23]. Comparing IR spectra of P25 and sulfated TiO_2 powders, two peaks at 1130 and 1057 cm^{-1} are observed for sulfated TiO_2 powders, but not for the P25 powders. These peaks are the characteristic frequencies of a bidentate SO_4^{2-} coordinated to metals such as Ti^{4+} [15]. Additionally, no absorbance bands in the range from 900 to 990 cm^{-1} which can be attributed to the surface adsorbed sulfate ions species [16,24] are observed. This suggests that nearly all the SO_4^{2-} species entered the network of TiO_2 [16].

In addition, there are no differences between sulfated TiO_2 treated (curve b) and untreated (curve c). Bands in the range 950–700 cm^{-1} assigned to different Ti-peroxo species [10] is not found, this is maybe limited by the detection resolution of IR. It is also noticed that the peaks at 1130 and 1057 cm^{-1} for the curve d assigned to the titania calcined at 450 °C for 1 h are weaker than that of curves a–c, i.e., some sulfate ions coordinate with TiO_2 in the network was decomposed during calcinations. This trend is even more obvious when TiO_2–400–2 (curve f) is checked, i.e., its peak at 1057 cm^{-1} which is usually assigned to active sulfate species [25] almost disappears completely. Therefore, the calcination at higher temperature is shown to be able to reduce the sulfate species coordinate with TiO_2 in the network, which leads the vis absorption of sulfated TiO_2 decreasing with the increase of calcination temperature and duration (Fig. 3a).

Fig. 5 shows the XPS spectra of the S_{2p} band for used samples. The BE of 168.7 eV suggests that the sulfur in sulfated TiO_2 exists in a six-oxidation state (S^{6+}) [15,26] as chelating bridging bidentate

microspores with the increase of calcination temperature and duration. So, it is believed that the structure change of sulfated TiO_2 plays an important role in increasing the surface area of sulfated TiO_2.

Some researchers report that the absorption becomes stronger as the surface area of TiO_2 powders increases [8,10]. However, what we found is somewhat contradicted to those observations. Fig. 3a and Table 1 show that the vis absorption becomes lower when the surface area of TiO_2 powders increases. What causes this? During the process of synthesizing sulfated TiO_2, sulfuric acid was added so that sulfate ions would be anchored on the surface of sulfated TiO_2 powders. We assume that these sulfate species are one of the most important factors that improve absorption in the visible part of the spectrum. Sulfate species usually start to decompose at only above 400 °C [22], so little decrease of vis absorption should be observed

Table 1
Crystallite phase, crystallite size and surface area for sulfated TiO_2 and P25.

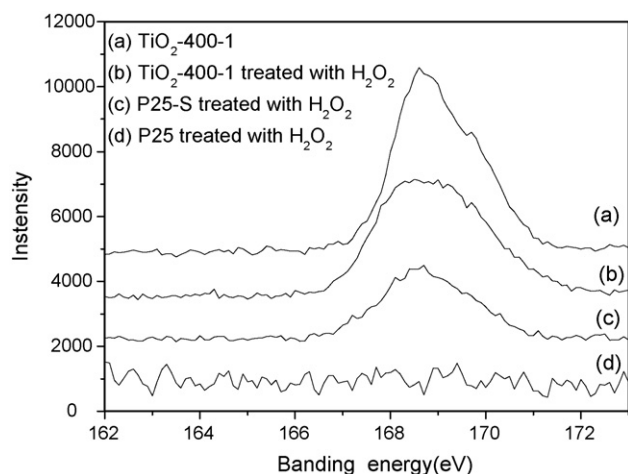| Samples	Crystalline phase	Crystalline size (nm)	S_{BET} (m^2 g^{-1})
TiO_2–350–1	Anatase	8	55.66
TiO_2–400–1	Anatase	8.1	59.75
TiO_2–400–2	Anatase	13.3	68.71
TiO_2–450–1	Anatase	10.1	65.12
P25	Anatase	23.7	49.29
	Rutile	–	
P25-S	Anatase	22.4	43.64
	Rutile	–	

Fig. 5. XPS spectra of the S_{2p} band of used samples.

complex [27]. This is consistent with the result of IR spectra in Fig. 4. For P25, no the S_{2p} band was observed. The molar ratio between S and Ti for the TiO_2–400–1 before and after treatment with H_2O_2 is 1:3.8 and 1:4.1, respectively, indicating that sulfate ions species are partly replaced by H_2O_2, resulting in the decrease of S content. However, for P25-S, the ratio is 1:10.8, which indicates that sulfate species anchored on P25-S is less than that on TiO_2–400–1.

The Ti_{2p} spectra for TiO_2–400–1 before the treatment with H_2O_2 consists of two peaks of $Ti_{2p3/2}$ and $Ti_{2p1/2}$ located at 459.1 and 464.9 eV (Fig. 6a), respectively, indicating that Ti ions are in an octahedral environment [28,29]. The electrons can strongly be withdrew from the neighboring Ti cations by bidentate sulfate formed on the surface of TiO_2, resulting in a slight increase of BE of the Ti cations [15]. This can be explained by the increase in effective positive charge around Ti surface species [30]. $Ti_{2p3/2}$ BE of the sulfated TiO_2 shifts from 458.4 eV for pure TiO_2 [30] to 459.1 eV. For TiO_2–400–1 sensitized with hydrogen peroxide (Fig. 6b), the band $Ti_{2p3/2}$ consists of two peaks at 458.7 and 460.5 eV with an atomic ratio of about 73:27, respectively, which implies the two different chemical environments of Ti ions exist in the sensitized titania structure: one in an octahedral coordination with oxygen, and the other in a tetrahedral environment [28,29]. The tetrahedral coordination for Ti ions with oxygen comes from the peroxo-titanium complexes due to the collaboration between peroxo groups and sulfate species. However, it is noticeable that nothing exists in P25 and P25-S except the Ti ions in an octahedral coordination with oxygen, although they both are sensitized with H_2O_2 (Fig. 6c). The tetrahedral environment of TiO_2 ions was reported more for phosphated TiO_2 [29] and SiO_2/TiO_2 composite [28,31]. Meanwhile, the formation of peroxo complexes can cause partial electron transformation from the neighboring Ti to peroxo groups and a decrease of the electron density on Ti, resulting in an increase of BE of the partial Ti cations to 460.5 eV, which is much more than that of TiO_2 sensitized with only H_2O_2 [31]. And then a decrease of BE of other Ti cations occurred from 459.1 eV for TiO_2–400–1 untreated with H_2O_2 to 468.7 eV for the treated due to countervail of electron withdrawing effect from both peroxo complexes and sulfate ions, which indicates the withdrawing electron effect is stronger for peroxo groups than sulfate species.

Peroxo groups could not be detected in the IR spectra of sulfated TiO_2 sensitized with H_2O_2 (Fig. 4). However, the band of peroxo groups can be easily observed in the XPS spectra. Fig. 7a shows the O_{1s} XPS spectrum of TiO_2–400–1 before treatment with H_2O_2. Peak separation of the O_{1s} spectrum clearly shows two kinds of oxygen with binding energies of 530.4, and 531.9 eV. The band at 530.4 eV is attributed to the Ti(IV)–O bonds [28,32]. The one at 531.9 eV is
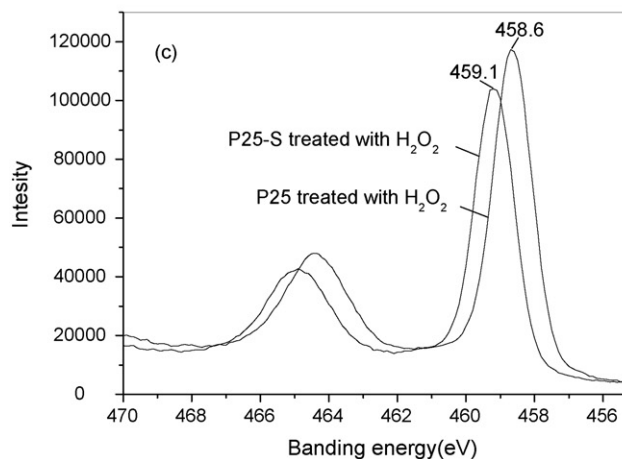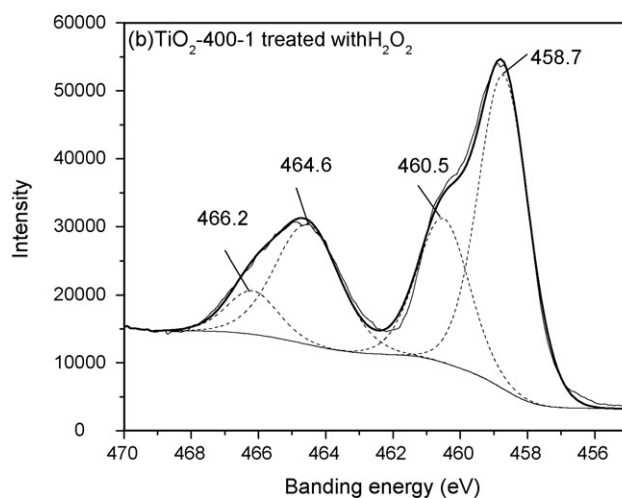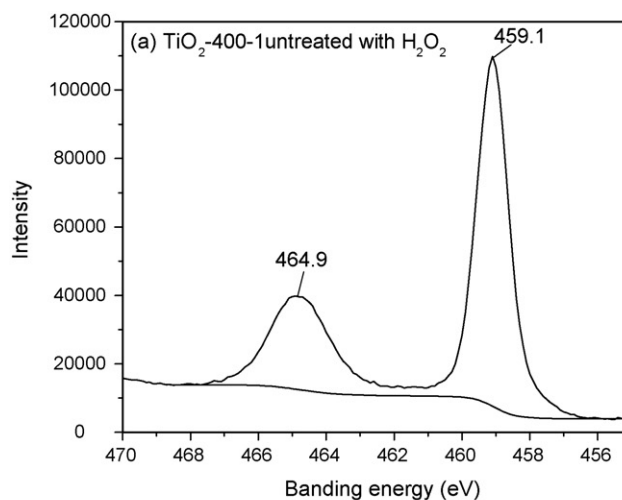

Fig. 6. XPS spectra of the Ti_{2p} band of used samples.

assigned to hydroxyl groups [32] due to absorbed water, as well as oxygen in sulfate [16,30], which was confirmed by IR in Fig. 4. Compared with titania untreated with H_2O_2, O_{1s} of treated titania can be separated into tree peaks (Fig. 7b), located at 530.1, 531.9 and 533.7 eV, respectively, which can be attributed to Ti–OH at 531.9 eV and Ti–O at 530.1 eV, and the new peak at 533.7 eV is assigned to peroxo groups [10,32], with proportion contributions of 8.8% (Table 2). And the peroxo groups also were observed for P25 and P25-S treated with H_2O_2, with proportion contributions of 6.1 and
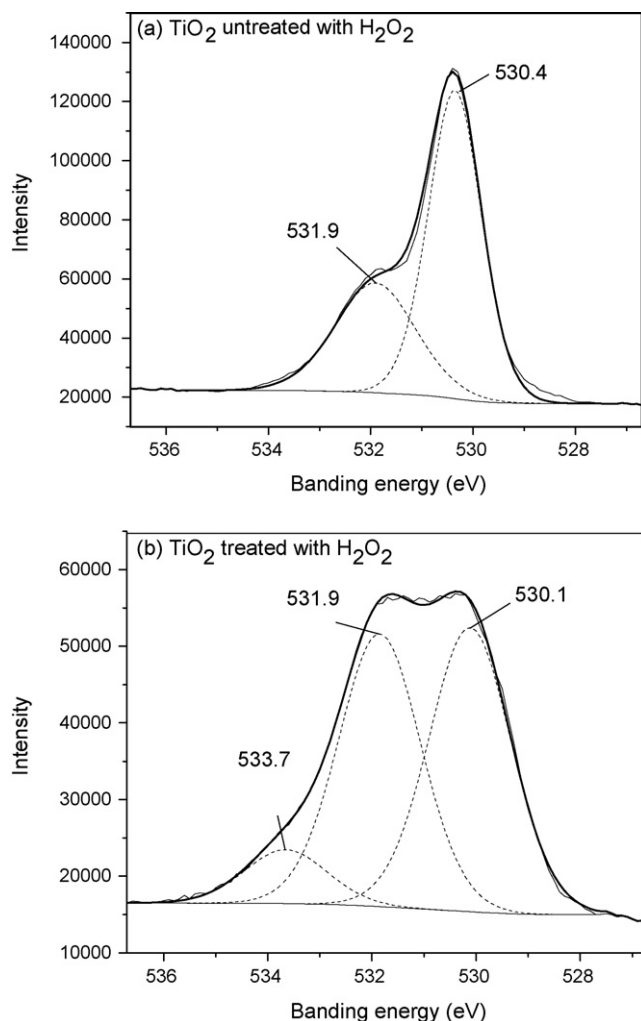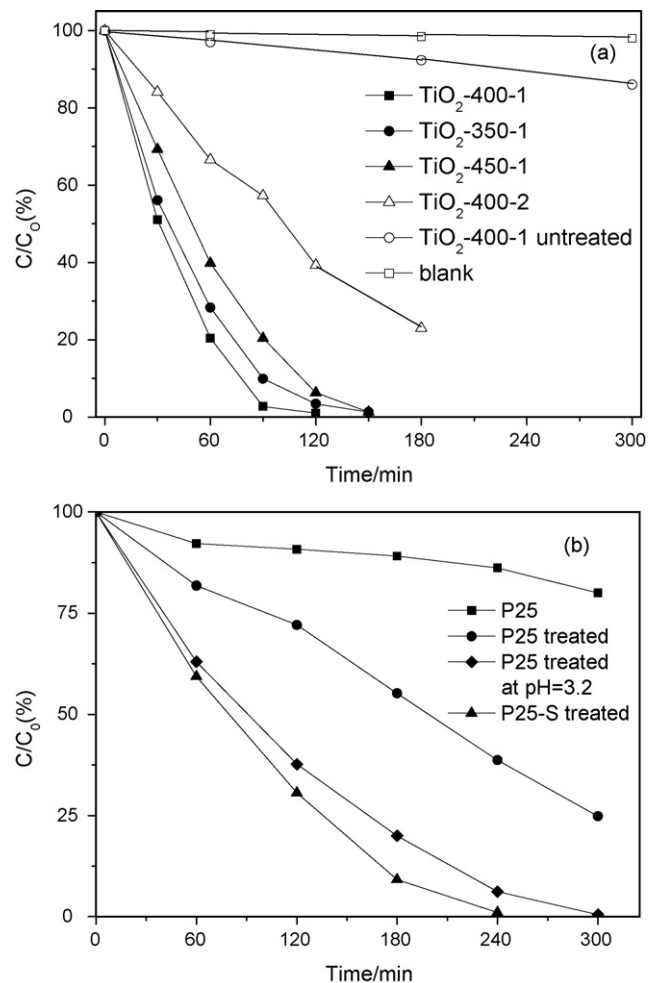
Fig. 7. XPS spectra of the O_{1s} band of $TiO_2-400-1$ untreated (a) and treated (b) with H_2O_2.

Fig. 8. Photocatalytic activities of sulfated TiO_2 (a) and P25 (b) sensitized with H_2O_2 under visible light ($\lambda > 420$ nm).

7.3%, respectively (Table 2). It is obvious that the band assigned to hydroxyl groups is stronger for the $TiO_2-400-1$ after the treatment with H_2O_2 (Fig. 7b) than that for $TiO_2-400-1$ untreated (Fig. 7a), as Ti ions in tetrahedral coordination can provide additional surface hydroxyl groups by adsorbed water in air [29]. Table 2 also shows the similar results, much more hydroxyl groups existing on the surface of $TiO_2-400-1$ with Ti ions in tetrahedral coordination than that on P25 and P25-S only with Ti ions in octahedral coordination.

3.4. Photocatalytic activity

Photocatalytic activity tests were conducted by the degradation of methyl orange in aqueous solution under visible light irradiation. Fig. 8a shows the results of photocatalytic degradation of MO water solution for nanosize titania. As can be seen, the blank sample, 200 mL MO solution containing 2 mL 30% H_2O_2, discolors MO only about 2% in 300 min, whereas the sample treated without H_2O_2

Table 2
Content for different type of oxygen atoms for used samples treated with H_2O_2.

Samples	Content for different type of oxygen atoms (%)		
	O–H and S–O	O–O	Ti–O
P25	15.6	6.1	78.3
P25-S	16	7.3	76.7
$TiO_2-400-1$	44.7	8.8	46.5

have about 15% discoloration. After sensitized with hydrogen peroxide, the samples can acquire up to 98% discoloration in 150 min except the $TiO_2-400-2$. The differences in calcination temperature can lead to different results of MO degradation. The $TiO_2-400-1$ has a best photocatalytic behavior, and 99% discoloration was acquired in just 120 min. Additionally, the prolongation of calcination time can decrease the photocatalytic activity of sulfated TiO_2, 2 h calcining at 400 °C resulting only 80% degradation of MO in 180 min. Compared the $TiO_2-400-1$ before and after treatment with H_2O_2, it is notable that the vis photocatalytic activity can be improved dramatically by H_2O_2, which is also supported by the observations in Fig. 8b. The degradation of MO increases from about 20% for P25 to 80% for one sensitized with peroxide hydrogen in 300 min. Therefore, it can be concluded that the degradation of MO for P25 is much lower than the one for sulfated titania under visible light irradiation.

Similarly, the pH value also influences the photoactivity of catalyst [33]. An enhancement in photoactivity was observed when P25 treated with only H_2O_2 were photoirradiated in a MO solution containing H_2SO_4 having pH value of 3.2 as $TiO_2-400-1$ suspensions (Fig. 8b). As for the increase of MO degradation in acidic solution, it was basically due to that acidic environment would enhance the adsorption strengths of the reactant dye MO [33,34], which was also supported by the observations in Fig. 9. However, according to Figs. 8b and 9, although P25-S suspensions had much lower adsorption than that in P25 suspensions at pH 3.2, the higher photoactivity was observed for P25-S. And an approximately 20% difference in adsorption strength could not also explain why MO degradation

Fig. 9. The adsorption rates of MO in used samples suspensions.

Fig. 10. Infrared spectra of pyridine molecules adsorbed on TiO_2–400–1 treated with H_2O_2 (a) and untreated (b) in the atmosphere (humidity 80%).

on TiO_2–400–1 was nearly as two times as that on P25 at pH 3.2. Those hinted that the adsorption of the reactant would be not solely responsible for the high photoactivity of sulfated TiO_2.

The surface sulfur complex anchored on the TiO_2 can produce strong electron-inducing effect. So, a large number of Brønsted and Lewis acidic sites were created on the surface of TiO_2 [35], indicating that the presence of active sulfate species on the surface of TiO_2 increased the surface acidity of TiO_2 [25,36]. The strong surface acidity would improve photocatalytic activity of TiO_2 [37], since photo-induced electrons could be captured by these acidic sites [16]. Meanwhile, higher content of active sulfate species and suitable crystallinity of TiO_2 should be the prerequisites for producing strong surface acidity [25]. Generally, sulfation of TiO_2 is carried out by calcining amorphous TiO_2 at high temperature (at least 500 °C) to get higher catalytic activities [18]. Unfortunately, high temperature may lead to the decomposition of a large amount of active sulfate species as indicated by the IR results in Fig. 4. In our study, the high temperature is dispensable because crystalline TiO_2 has been produced in the hydrolysis process. Hereby, strong surface acidity for sulfated TiO_2 can be obtained. In order to detect surface acidic sites for sulfated TiO_2 before and after treatment with H_2O_2, the chemisorptive states of pyridine molecules were examined by FT-IR in the atmosphere (Fig. 10), for photocatalytic reactions generally occurred at ambient conditions [15]. Since the Lewis acidic sites react with H_2O molecules and are converted to Brønsted acidic sites, only Brønsted acidic sites are observed for TiO_2–400–1, but a weak peak corresponding to Lewis acidic sites at 1448 cm^{-1} [36] is observed for TiO_2–400–1 after treatment with H_2O_2, which indicates Lewis acidic sites can be stabilized by H_2O_2.

Moreover, more surface chemisorptions centers for some reactants can be facilitated due to surface acidic sites [17]. We think these chemisorptions centers also serve hydrogen peroxide. The sulfated TiO_2 sensitized with H_2O_2 can adsorb more hydrogen peroxide to form more peroxo-titanium complexes, resulting in more intensive vis absorption, which is the prerequisite for photocatalytic activity under visible light irradiation. The least active sulfate species anchor on TiO_2–400–2 (Fig. 4), which corresponds to the lowest vis absorption (Fig. 3a). It is also supported by the more intensive absorption of P25-S in the visible light region (Fig. 3b), although its surface area is lower than that of P25 (Table 1). In addition, based on the XPS analysis, the stronger withdrawing effect of peroxo groups to electrons can increase the charge of Ti surface species, which can hinder recombination of photogenerated electrons and holes [30].
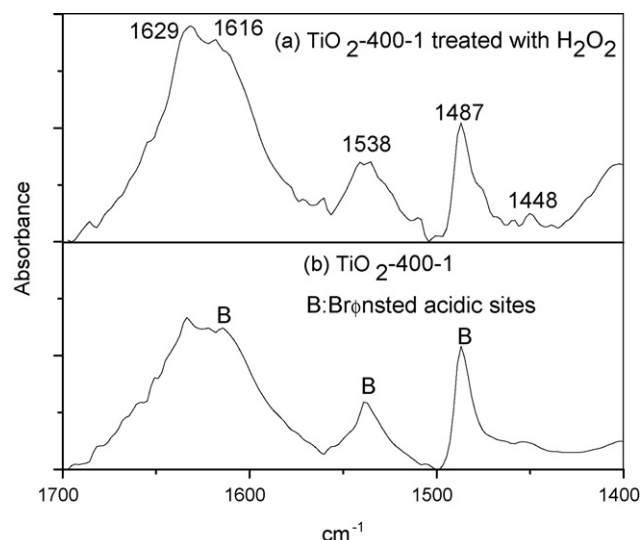
Additionally, as discussed above based on Figs. 6 and 7, Ti ions in tetrahedral coordination, coming from the collaboration between sulfate species and peroxo groups, can provide additional surface hydroxyl groups. These surface hydroxyl groups can stabilize the photoexcited hole and electron pairs [25,38] and react with photoexcited holes on the catalyst surface to produce hydroxyl radicals proven to be powerful oxidants in degrading organics [39]. Meanwhile, Wang et al. [15] reported the high density of surface hydroxyl groups could improve the chemisorption capability of TiO_2 surfaces toward reactant molecules, such as O_2, and the increase in the oxygen adsorption is proportional to the interfacial transfer of photoexcited electrons. Furthermore, the Lewis acidic sites for sulfated TiO_2 sensitized with H_2O_2 can initiate the water photooxidation [40] and the photocatalytic oxidation of organic compounds on TiO_2 under visible light mainly proceed via reactions with surface intermediates of water oxidation or oxygen reduction [41].

4. Conclusions

In this paper, the anatase TiO_2 nanoparticles were prepared by the sulfuric-acid-catalyzed hydrolysis of boiling $TiCl_4$ solutions. The high content of active sulfate species and suitable crystallinity for sulfated TiO_2 were acquired by calcining at lower temperature, resulting in strong surface acidity. After sensitized with hydrogen peroxide, the sulfated titania powders exhibit much higher vis photocatalytic activity relative to P25 powders. We conclude that the outstanding vis activity of sulfated TiO_2 sensitized with H_2O_2 is related to the existence of large amount acidic sites due to sulfate ion species, Ti ions in a tetrahedral coordination and strong vis absorption.

Acknowledgment

References

[1] D. Dvoranova, V. Brezova, M. Mazur, M. Malati, Investigations of metal-doped titanium dioxide photocatalysts, Appl. Catal. B 37 (2002) 91–105.
[2] R. Asahi, T. Morikawa, T. Ohwaki, A. Aoki, T. Taga, Visible-light photocatalysis in nitrogen-doped titanium oxides, Science 293 (2001) 269–271.

[3] A.S. Polo, M.K. Itokazu, N.Y.M. Iha, Metal complex sensitizers in dye-sensitized solar cells, Coord. Chem. Rev. 248 (2004) 1343–1361.

[4] S. Pavasupree, Y. Suzuk, S. Pivsa-Art, Preparation and characterization of mesoporous TiO_2–CeO_2 nanopowders respond to visible wavelength, J. Solid State Chem. 178 (2005) 128–134.

[5] S. Kim, W. Choi, Visible-light-induced photocatalytic degradation of 4-chlorophenol and phenolic compounds in aqueous suspension of pure titania: demonstrating the existence of a surface-complex-mediated path, J. Phys. Chem. B 109 (2005) 5143–5149.

[6] W. Chu, C.C. Wong, The photocatalytic degradation of dicamba in TiO_2 suspensions with the help of hydrogen peroxide by different near UV irradiations, Water Res. 38 (2004) 1037–1043.

[7] M.A. Barakat, J.M. Tseng, C.P. Huang, Hydrogen peroxide-assisted photocatalytic oxidation of phenolic compounds, Appl. Catal. B 59 (2005) 99–104.

[8] H. Boonstra, C.H.A. Mutsaers, Adsorption of hydrogen peroxide on the surface of titanium dioxide, J. Phys. Chem. 79 (1975) 1940–1943.

[9] X.Z. Li, C.C. Chen, J.C. Zhao, Mechanism of photodecomposition of H_2O_2 on TiO_2 surfaces under visible light irradiation, Langmuir 17 (2001) 4118–4122.

[10] T. Ohno, Y. Masaki, S. Hirayama, M. Matsumura, TiO_2-photocatalyzed epoxidation of 1-decene by H_2O_2 under visible light, J. Catal. 204 (2001) 163–168.

[11] Y.K. Takahara, Y. Hanada, T. Ohno, S. Ushiroda, S. Ikeda, Photooxidation of organic compounds in a solution containing hydrogen peroxide and TiO_2 particles under visible light, J. Appl. Electrochem. 35 (2005) 793–797.

[12] T. Hirakawa, K. Yawata, Y. Nosaka, Photocatalytic reactivity for $O_2^{•-}$ and $OH^{•}$ radical formation in anatase and rutile TiO_2 suspension as the effect of H_2O_2 addition, Appl. Catal. A 325 (2007) 105–111.

[13] T. Hirakawa, Y. Nosaka, Properties of $O_2^{•-}$ and $OH^{•}$ formed in TiO_2 aqueous suspensions by photocatalytic reaction and the influence of H_2O_2 and some ions, Langmuir 18 (2002) 3247–3254.

[14] M.R. Hoffmann, S.T. Martin, W. Choi, D.W. Bahnemann, Environmental applications of semiconductor photocatalysis, Chem. Rev. 95 (1995) 69–96.

[15] X.C. Wang, J.C. Yu, P. Liu, X.X. Wang, W.Y. Su, Probing of photocatalytic surface sites on SO_4^{2-}/TiO_2 solid acids by in situ FT-IR spectroscopy and pyridine adsorption, J. Photochem. Photobiol. A 179 (2006) 339–347.

[16] H.X. Li, G.S. Li, J. Zhu, Y. Wan, Preparation of an active SO_4^{2-}/TiO_2 photocatalyst for phenol degradation under supercritical conditions, J. Mol. Catal. A 226 (2005) 93–100.

[17] D.S. Muggli, L. Ding, Photocatalytic performance of sulfated TiO_2 and Degussa P-25 TiO_2 during oxidation of organics, Appl. Catal. B 32 (2001) 181–194.

[18] F. Jiang, Z. Zheng, Z.Y. Xu, S.R. Zheng, Z.B. Guo, L.Q. Chen, Aqueous Cr(VI) photoreduction catalyzed by TiO_2 and sulfated TiO_2, J. Hazard. Mater. 134 (2006) 94.

[19] X.Z. Fu, Z. Ding, W. Su, Structure of titania-based solid superacids and their properties for photocatalytic oxidation, Chin. J. Catal. 20 (1999) 321–324.

[20] Q.H. Zhang, L. Gao, J.K. Guo, Effect of hydrolysis conditions on morphology and crystallization of nanosized TiO_2 powder, J. Eur. Ceram. Soc. 20 (2000) 2153–2158.

[21] Y.F. Zhang, Y. Wei, Z.H.B. Jia, M.J. Han, P. Wang, Preparation of nanocrystal TiO_2 with rutile structure at lower temperature from $TiOCl_2$ solution, J. Inorg. Mater. 16 (2001) 1217.

[22] G. Colón, M.C. Hidalgo, J.A. Navıo, Photocatalytic behaviour of sulphated TiO_2 for phenol degradation, Appl. Catal. B 45 (2003) 39–50.

[23] Z.G. Ding, Q. Lu, P.F. Greenfield, Role of the crystallite phase of TiO_2 in heterogeneous photocatalysis for phenol oxidation in water, J. Phys. Chem. B 104 (2000) 4815–4820.

[24] T. Jin, M. Machida, T. Yamaguchi, K. Tanabe, Infrared study of sulfur-containing iron oxide. Behavior of sulfur during reduction and oxidation, Inorg. Chem. 23 (1984) 4396–4398.

[25] Q. Yang, Ch. Xie, Z. Xu, Z. Gao, Y. Du, Synthesis of highly active sulfate-promoted rutile titania nanoparticles with a response to visible light, J. Phys. Chem. B 109 (2005) 5554–5560.

[26] Y. Okamoto, M. Oh-Hara, A. Maezawa, T. Imanaka, S. Teranishi, Hydrogen sulfide adsorption on alumina, modified alumina, and molybdenum trioxide/alumina, J. Phys. Chem. 90 (1986) 2047–2396.

[27] S.T. Choo, Y.G. Lee, I.S. Nam, S.W. Ham, J.B. Lee, Characteristics of V_2O_5 supported on sulfated TiO_2 for selective catalytic reduction of NO by NH_3, Appl. Catal. A 200 (2000) 177–188.

[28] A.A.S. Alfaya, Y. Gushikem, Highly dispersed phosphate supported in a binary silica–titania matrix: preparation and characterization, Chem. Mater. 10 (1998) 909–913.

[29] J.C. Yu, L.Z.H. Zhang, Z. Zheng, J.C. Zhao, Synthesis and characterization of phosphated mesoporous titanium dioxide with high photocatalytic activity, Chem. Mater. 15 (2003) 2280–2286.

[30] E. Barraud, F. Bosc, D. Edwards, N. Keller, Gas phase photocatalytic removal of toluene effluents on sulfated titania, J. Catal. 235 (2005) 318–326.

[31] X.H. Shu, Y. Chen, H.Y. Yuan, S.F. Gao, D. Xiao, H_2O_2 sensor based on the room-temperature phosphorescence of nano TiO_2/SiO_2 composite, Anal. Chem. 79 (2007) 3695–3702.

[32] Y.F. Gao, Y. Masuda, K. Koumoto, Light-excited superhydrophilicity of amorphous TiO_2 thin films deposited in an aqueous peroxotitanate solution, Langmuir 20 (2004) 3188–3194.

[33] I.K. Konstantinou, T.A. Albanis, TiO_2-assisted photocatalytic degradation of azo dyes in aqueous solution: kinetic and mechanistic investigations, Appl. Catal. B 49 (2004) 1–14.

[34] K.M. Parida, N. Sahu, N.R. Biswal, B. Naik, A.C. Pradhan, Preparation, characterization, and photocatalytic activity of sulfate-modified titania for degradation of methyl orange under visible light, J. Colloid Interf. Sci. 318 (2008) 231–237.

[35] X.Zh. Fu, W.A. Zeltner, Q. Yang, M.A. Anderson, Catalytic hydrolysis of dichlorodifluoromethane (CFC-12) on sol–gel-derived titania unmodified and modified with H_2SO_4, J. Catal. 168 (1997) 482–490.

[36] L.K. Noda, R.M. Almeida, N.S. Goncalves, L.F.D. Probst, O. Sala, TiO_2 with a high sulfate content—thermogravimetric analysis, determination of acid sites by infrared spectroscopy and catalytic activity, Catal. Today 85 (2003) 49–69.

[37] J. Papp, S. Soled, K. Dwight, A. Wold, Surface acidity and photocatalytic activity of TiO_2, WO_3/TiO_2, and MoO_3/TiO_2 photocatalysts, Chem. Mater. 6 (1994) 496–500.

[38] S.J. Tsai, S. Cheng, Effect of TiO_2 crystalline structure in photocatalytic degradation of phenolic contaminants, Catal. Today 33 (1997) 227–237.

[39] J.C. Yu, J. Lin, R.W.M. Kwok, Enhanced photocatalytic activity of $Ti_{1-x}V_xO_2$ solid solution on the degradation of acetone, J. Photochem. Photobiol. A 111 (1997) 199–203.

[40] R. Nakamura, Y. Nakato, Primary intermediates of oxygen photoevolution reaction on TiO_2 (rutile) particles, revealed by in situ FTIR absorption and photoluminescence measurements, J. Am. Chem. Soc. 126 (2004) 1290–1298.

[41] R. Nakamura, T. Tanaka, Y. Nakato, Mechanism for visible light responses in anodic photocurrents at N-doped TiO_2 film electrodes, J. Phys. Chem. B 108 (2004) 10617–10620.